Direct Determination of Energy Level Alignment and Charge Transport at Metal-Alq_{3} Interfaces via Ballistic-Electron-Emission Spectroscopy

J. S. Jiang, J. E. Pearson, and S. D. Bader

Phys. Rev. Lett. **106**, 156807 — Published 14 April 2011

DOI: 10.1103/PhysRevLett.106.156807

Direct Determination of Energy Level Alignment and Charge Transport at Metal/Alq_3 Interfaces via Ballistic-Electron-Emission Spectroscopy

J. S. Jiang,* J. E. Pearson, and S. D. Bader

Materials Science Division, Argonne National Laboratory, Argonne, IL 60439

Abstract

The energy level alignment at the interfaces between metals and the archetypal electroluminescent organic semiconductor tris-(8-hydroxyquinoline) aluminum (Alq_3) has long been controversial, and the interpretation of charge transport in Alq_3-based devices is often complicated by uncertainties in interfacial characteristics. Using ballistic-electron-emission spectroscopy (BEES), we directly determined the energy barrier for electron injection at clean interfaces of Alq_3 with Al and Fe to be 2.1 eV and 2.2 eV, respectively. We quantitatively modeled the sub-barrier BEES spectra with an accumulated space charge layer, and found that the transport of non-ballistic electrons is consistent with random hopping over the injection barrier.

PACS numbers: 71.20.Rv, 73.61.Ph, 73.40.-c, 73.40.Gk

Dramatic progress has been made in organic electronics, where organic-based devices are rivaling those based on conventional inorganic semiconductors.[1] Presently, efforts are underway to apply spintronic principles[2], which originated from inorganic materials, to carbon nanotubes, molecular monolayers, and bulk organic semiconductors for a new class of organic electronics that exploit the spin of charge carriers.[3] However, the field of organic electronics also has a history of concerns that new phenomena may be artifacts caused by extrinsic, and ill-defined, defects, rather than by the intrinsic properties of the molecular species under study.[4] There is a controversy over whether the reported magnetoresistance in organic spin-valve devices indeed results from injection and coherent transport of spins on molecular levels.[5] These devices[6] consist of a nominally thick organic semiconductor layer (*e.g.* Alq_3) sandwiched between two ferromagnetic metal (FM) electrodes; but their qualification as spin valves has been challenged, because similar devices indicate direct tunneling through structural non-uniformities rather than molecular transport, and because low hole mobility in truly non-tunneling devices prevents efficient spin injection in the first place.[7–9] Recent experiments have been designed to counter these challenges, but they raise new questions of their own. Muon spin rotation measurements[11] appeared to show spin diffusion in Alq_3 organic light-emitting diodes (OLED) with FM electrodes; but little-noticed is the LiF layer inserted between the electrode and Alq_3. LiF is known to release Li atoms, which readily diffuse and react with Alq_3 to become part of the cathode.[12] It is not clear whether the reported spin diffusion is the latent distribution of Li dopant or the carrier spin in the Alq_3 layer proper, notwithstanding that a previous study[10] found no spin polarization in similar OLEDs. Sun *et al.*[13] attempted to minimize metal-Alq_3 reaction using buffer-layer-assisted growth, and reported that their Co/Alq_3/$La_{0.67}Sr_{0.33}MnO_3$ (LSMO) devices had sharper interfaces and yielded a giant magnetoresistance. Yet they describe the device characteristics with a space-charge-limited current model, which is applicable only when ohmic contacts are formed between the electrode and organic semiconductor—usually by using low work function electrodes, or via doping or chemical damage.

More importantly, the state of confusion over spin transport in organic media underscores a larger issue: gaps in understanding the properties of metal/organic interfaces have become impediments to properly describing the basic physics of charge transport in organic-based devices, and to employing organics as active materials in new frontiers of science. Despite Alq_3 being an archetypal organic electroluminescent material, interpretations of the charge

transport characteristics in Alq_3 devices vary dramatically in the literature.[14] Differences in material and preparation conditions and interface characteristics can contribute to the discrepancies.[14–16] Wolf *et al.*[17] pointed out that the injection barrier height (Δ), *i.e.* the difference between the electrode Fermi Level (ϵ_F) and the organic's lowest unoccupied molecular orbital (LUMO) or highest occupied molecular orbital (HOMO), is a crucial parameter in determining the nature of charge transport in organic electronic devices. However, while the HOMO level and vacuum level offset can be reliably determined from ultraviolet photoemission spectroscopy (UPS),[18] it is generally understood that the conventional approach of estimating LUMO by adding the optical gap to the HOMO level neglects excitonic effects.[16, 19, 20] Unfortunately, different experimental techniques to directly measure LUMO have their own caveats and yield conflicting results. The Alq_3 HOMO-LUMO gap was determined to be 4.6 eV by inverse photoelectron spectroscopy (IPES)[19], but was given as 2.96 eV from scanning tunneling spectroscopy (STS)[20]. Zhan *et al.*[21] constructed an energy level diagram that favored electron injection from Co and LSMO into Alq_3 by choosing the Alq_3 HOMO-LUMO gap determined from STS over that from IPES. They argued that IPES could have caused sample modifications with strong electron fluxes, although reports[22, 23] exist that a scanning tunneling microscope (STM) tip might do just the same.

Ballistic Electron Emission Spectroscopy (BEES) is an established technique for characterizing the band structure at metal/inorganic semiconductor interfaces.[24] It was recently extended to measure Δ at metal/organic interfaces.[22, 23] A schematic diagram of the BEES technique is shown in Fig. 1(a). Ballistic electrons tunnel from an emitter into a thin metal base in contact with an organic semiconductor; they can enter the LUMO if their energy exceeds Δ. Since the energy of the electrons is the potential difference between the base and emitter (V_{BE}), Δ is simply the threshold V_{BE} at which the collector current (I_C) rises sharply. The emitter can be the tip of an STM, or an all-solid-state tunnel junction. The STM implementation offers spatial resolution, but there are concerns about the stability of the spectra and measurement-induced sample modifications.[22, 23] STM-based BEES is also limited to interfaces where the base is on top of the organic. Since metal deposition onto organics tends to create interfacial gap states,[12, 16] care must be taken when associating the injection threshold in STM-based BEES with true molecular levels.

In the present work, we applied BEES to directly determine the electron injection barrier

at metal/Alq_3 interfaces. We used large-area (compared to a STM-tip) Al_2O_3 tunnel junctions for injecting ballistic electrons, and placed the emitter under the base so that Alq_3 was deposited on top of the metal in order to achieve clean and stable metal/Alq_3 interfaces. Whereas in conventional BEES the sub-barrier I_C is considered leakage and is ignored, we quantitatively modeled the sub-barrier BEES spectra with an accumulated space charge layer from ballistic injection. The presence of the space charge allowed us to distinguish between the usual organic charge injection mechanisms. We show that non-ballistic charge injection at clean metal/Alq_3 interfaces is limited by random hopping of carriers from ϵ_F over the injection barrier, and that there also exist uniformly-distributed gap states on which charge carriers can be transported.

We fabricated the Alq_3 BEES devices in a high-vacuum cluster deposition system[8] via thermal evaporation and shadow masking. The vacuum pressure during evaporations was $< 1 \times 10^{-8}$ Torr; sample transfers between deposition chambers and mask changes were performed without breaking the vacuum. The emitter structure always consisted of an Al electrode and an Al_2O_3 tunnel barrier. We used Al or Fe for the base, and Al or Au for the collector. In the following, we will denote a device by the materials in its base-collector structure, *e.g.* Fe/Alq_3/Au for a device with an Fe base, an Alq_3 spacer and a Au collector. Shown in Fig. 1(b) is an optical micrograph of an Al/Alq_3/Al device. The 12-nm thick Al emitter was first evaporated through a 20-μm wide slit in a mask on the SiN substrate. It was oxidized by *in situ* plasma-assisted oxidation to form the Al_2O_3 tunnel barrier. A 4-nm thick, 200-μm wide base electrode was subsequently deposited at 45° with the emitter to complete the emitter-base tunnel junction. The 100-nm Alq_3 layer covered the entire sample. Finally, the 10-nm thick collector electrode was deposited through a 100-μm wide mask, perpendicular to the base electrode. The device thus had an emission area (A_e) of $1.4 \times 10^3 \mu m^2$, and a collection area of $2.0 \times 10^4 \mu m^2$.

The room-temperature BEES measurements were carried out with the devices sealed in darkness. Because of the large thickness and the relatively poor mobility of carriers in Alq_3, it was necessary to apply a base-collector bias (V_{CB}) to attain a measurable I_C. At each V_{CB} value, V_{BE} was ramped stepwise, and I_C was measured in the steady state. The *rms* noise level of our setup is ∼100 fA. The devices were stable over repeated cycling of V_{CB} and V_{BE}; they failed only when we unknowingly ramped V_{BE} past dielectric breakdown of the tunnel junctions. Since we limited the measurement polarity to electron-injection only,

there was no issue of Alq_3 degradation from unbalanced hole injection[8, 25].

Shown in Fig. 1(c) is the emitter current (I_E) as a function of V_{BE} for the emitter tunnel junction in an Al/Alq_3/Al device. I_E rises monotonically with V_{BE}. The collector current due to ballistic injection, $\Delta I_C = I_C(V_{BE}) - I_C(0)$, is plotted in Fig. 1(d) for several values of V_{CB}. At small V_{CB} (< 4 V), ΔI_C initially increases slowly with V_{BE}, but rises much faster at higher V_{BE}, as is expected when ballistic electrons have sufficient energy to overcome the injection barrier and enter the Alq_3 LUMO. However, when $V_{CB} \geq 4$ V, a striking feature is seen: ΔI_C actually decreases initially, before rising sharply at higher V_{BE}; it appears that the injection of ballistic electrons hampers the charge transport in the Alq_3 layer. To our knowledge, this effect has not been reported in any BEES study. From the position of the ΔI_C minima, which remains constant for all values of V_{CB}, we determine Δ to be $2.10 \pm 0.05V$ for electron injection at the Al/Alq_3 interface. A constant injection barrier height indicates that the image charge effect is absent. This could be because the relaxation time for high-energy (> 2 eV) ballistic electrons ($\sim$20 fs [26]) is far shorter than the minimum polaronic hopping time ($\sim$100 fs [15]); the image hole left behind by a ballistic electron is already filled before the electron hops onto the next molecular site.

Figure 1(e) shows the zero-emission collector current, $I_C(0)$, as a function of V_{CB}. This non-ballistic electron current injected from the Al base via the application of V_{CB} is precisely the usual charge current in a Al/Alq_3/Al device. Comparing our results with those in the literature, we find that the current density in our device is about two orders of magnitude smaller than that in a similar device in Ref. [15], but is very similar to that in the Alq(2) device of Ref. [14] under reverse bias. The device in Ref. [15] had Al grown on Alq_3, which likely had chemical reactions at the interface, making it appropriate to describe injection as a process of charge hopping out of the reacted interfacial sites. On the other hand, both ours and the device of Ref. [14] had Alq_3 grown on Al, which led to cleaner and more ideal interfaces, and thus a different charge injection mechanism.

Arkhipov *et al.* [27] modeled charge injection from metals into organics as thermally-assisted hopping of carriers from the metal Fermi level onto a Gaussian distribution of molecular levels, followed by either recombination or diffusive escape. The hopping injected current (I_{hop}) is a function of Δ and the applied electric field (F). Taking $\Delta = 2.1$ eV, and the accepted literature values [15] for the bulk distribution width ($\sigma = 0.13$ eV) and inter-molecular distance ($a = 1$ nm), we fitted the data points in Fig. 1(e) to the Arkhipov

model and obtained $\gamma = 1.3$ nm^{-1} for the inverse localization radius. Since the injected charge binds with the Alq_3 molecule to form a polaron, it is reasonable that γ is close to $1/a$.

We model the sub-barrier BEES spectra by considering what happens when ballistic electrons with energy less than Δ are emitted into the base. Because of the energetic disorder in Alq_3, some of these ballistic electrons can enter the molecular sites and accumulate near the base/Alq_3 interface. For a layer of space charge located at $x = a$ with a density of n, along with the induced quasi-static image charge in the base and collector electrodes, the additional electrostatic potential created in the Alq_3 layer is:

$$V_{SC} = \begin{cases} \dfrac{ena}{\varepsilon\varepsilon_0}(1 - \dfrac{a}{L})x \equiv F_1 x & x \leq a, \\ \\ \dfrac{ena}{\varepsilon\varepsilon_0}(\dfrac{a}{L})(L - x) \equiv V_0 - F_2 x & x > a, \end{cases} \tag{1}$$

where x is the distance from the base electrode, ε is the dielectric constant, ε_0 is the vacuum permitivity, and L is the Alq_3 thickness.

At $x \leq a$, the space charge layer creates a retarding field F_1 towards base electrode. In the steady state, due to charge conservation, the drifting of the accumulated electrons back to the base electrode under F_1 mostly cancel the ballistic current impinging upon the base/Alq_3 interface. Therefore,

$$A_e ne\mu(F_1)F_1 = I_E \exp(-t/\lambda), \tag{2}$$

where t is the base electrode thickness, μ is the Poole-Frenkel field-dependent mobility as determined in Ref. [14], and the hot-electron attenuation length λ is ~ 10 nm [28] for Al. Solving Eqs. (1) and (2), we obtain n and plot it as a function of V_{BE} in Fig. 2(a). Assuming single occupancy, 0.45% of the Alq_3 molecules in the first layer is charged at $V_{BE} = 2$ V.

At $x > a$, the space charge layer raises the injection barrier by V_0, and the electric field in Alq_3 by F_2. The increased injection barrier impedes the hopping injection and reduces I_C. Since V_0 is much smaller than σ ($V_0 = 23$ mV at $V_{BE} = 2$ V), variations in V_0 due to disorder in the first Alq_3 layer do not affect I_C significantly.

On the other hand, some ballistically-injected electrons also contribute to I_C. At the tail of the Gaussian LUMO distribution, the transport levels can be considered uniform in density. The ballistically-injected electrons likely travel on all levels whose energies are less

than V_{BE}, the contribution to I_C being proportional to V_{BE}. Consequently, ΔI_C can be written as:

$$\Delta I_C = [I_{hop}(\Delta + V_0, F + F_2) - I_{hop}(\Delta, F)] + CV_{BE}. \quad (3)$$

The ΔI_C curves in Fig. 1(d) are fitted to Eq (3), with C as the sole fitting coefficient. In Fig. 2(b), we plot C as a function of V_{CB}. At low V_{CB}, C is nearly constant, suggesting that the transport is driven by diffusion, rather than by drift. At $V_{CB} \geq 5$ V, C increases sharply. The increased transport of ballistically-injected electrons overcomes the space charge-induced decrease in I_{hop} such that at $V_{CB} = 6$ V, ΔI_C always increases with V_{BE}. Comparing C at high V_{CB} with the expression for charge current under a uniform distribution of traps $J \propto V_{CB} \exp(2\varepsilon\varepsilon_0 V_{CB}/N_n kTeL^2)$[29], we estimated a trap density N_n of $\sim 5 \times 10^{23}$ $(\mathrm{m}^3 \cdot eV)^{-1}$. It has been suggested that electrons in Alq_3 are self-trapping [30], *i.e.* the total trap density equals the molecular density, the estimated N_n value represents the trap density at $\sim 4\sigma$ away from the center of the LUMO distribution.

Shown in Fig. 3(a) are I_C and dI_C/dV_{BE} plotted against V_{BE} for an Fe/ Alq_3/Au BEES device. From these curves, we obtain $\Delta = 2.2 \pm 0.1$ eV for electron injection from Fe into Alq_3. In Fig. 3(b), we show the schematic energy-level diagrams for Al/Alq_3 and Fe/Alq_3 interfaces. The difference between the Al ϵ_F and Alq_3 HOMO level was determined to be 2.7 eV via UPS.[18] Combining it with our BEES-determined $\Delta = 2.1$ eV, we arrive at a value of 4.8 eV for the Alq_3 HOMO-LUMO gap, which is in close agreement with the peak-to-peak gap [19] obtained via IPES. Given that the HOMO-ϵ_F differences for Co/Alq_3 and LSMO/Alq_3 interfaces were measured via UPS[21] as 2.1 eV and 1.7 eV respectively, the electron injection barriers are 2.7 eV and 3.1 eV at these interfaces. Such large barriers would make it highly unlikely that Co/Alq_3/LSMO spin-valve devices can have electron transport. We note, however, that the electron injection barriers determined via BEES are significantly higher than those defined from the bottom edges of the LUMO features in IPES [31]. In BEES, the upturn in I_C signifies ballistic electrons having sufficient energy to reach the collector electrode via the transport level; the lower-energy electrons, which enter the bottom edge of the LUMO distribution, are mostly reflected or become trapped, and are thus not transported through the thickness of the organic layer. Therefore, the different results from BEES and IPES highlight the need to properly define the injection barrier when examining charge transport in organic electronic devices.

The BEES technique has not been commonly employed to characterize molecular mate-

rials. By quantitatively modeling the sub-barrier BEES spectra, we have shown that it is a reliable method for directly determining the LUMO level. STM-based BEES has issues with spectra and sample stability; those concerns can however be alleviated in large-area tunnel junction-based BEES devices. More importantly, the basic scheme of BEES has been used to inject spin-polarized hot-electrons from tunnel junction emitters into inorganic semiconductors, exploiting the spin-filtering effect of the FM base.[32] A BEES device with FM base and collector electrodes would be an ideal structure for directly examining spin coherence in molecular materials.

In summary, we have determined the electron injection barriers at clean Fe/Alq_3 and Al/Alq_3 interfaces using ballistic-electron-emission spectroscopy. By exploiting the interaction between the ballistic and non-ballistic carriers, we were able to distinguish between charge injection mechanisms at the metal/Alq_3 interface. The transport of non-ballistic electrons is consistent with random hopping over the interfacial energy barrier.

Work supported by U.S. Department of Energy Office of Science, Basic Energy Sciences, under Contract No. DE-AC02-06CH11357.

---

* jiang@anl.gov

[1] S. R. Forrest, Nature, **428**, 911 (2004).

[2] S. A. Wolf *et al.* Science **294**, 1488 (2001).

[3] W. J. M. Naber, S. Faez, W. G. van der Wiel, J. Phys. D: Appl. Phys. **40**, R205 (2007).

[4] R. F. Service, Science, **302**, 556 (2003).

[5] G. Szulczewski, S. Sanvito and M. Coey, Nature, **8**, 693 (2009).

[6] Z. H. Xiong, D. Wu, Z. V. Vardeny, and J. Shi, Nature, **427**, 821 (2004).

[7] W. Xu *et al.* Appl. Phys. Lett. **90**, 072506 (2007).

[8] J. S. Jiang, J. E. Pearson, S. D. Bader, Phys. Rev. B **77**, 035303 (2008).

[9] H. Vinzelberg *et al.* J. Appl. Phys. **103**, 093720 (2008).

[10] G. Salis, S. F. Alvarado, M. Tschudy, T. Brunschwiler, R. Allenspach, Phys. Rev. B **70**, 085203 (2004).

[11] A. J. Drew *et al.* Nat. Mater, **8**, 109, (2009).

[12] M. G. Mason *et al.* J. Appl. Phys. **89**, 2756 (2001).

[13] D. Sun *et al.* Phys. Rev. Lett. **104**, 236602 (2010).

[14] W. Brütting, S. Berleb, A. G. Mückl, Org. Electron. **2**, 1, (2001).

[15] M. A. Baldo, S. R. Forrest, Phys. Rev. B **64**, 085201 (2001).

[16] J. C. Scott, J. Vac. Sci. Tech, A **21**, 521 (2003).

[17] U. Wolf, S. Barth, H. Bässler, Appl. Phys. Lett. **75**, 2035 (1999).

[18] H. Ishii, K. Sugiyama, E. Ito, K. Seki, Adv. Mater. **11**, 605 (1999).

[19] I. G. Hill, A. Kahn, Z. G. Soos, R. A. Pascal, Chem. Phys. Lett. **327**, 181 (2000).

[20] S. F. Alvarado, L. Rossi, P. Muller, P. F. Seidler, W. Riess, IBM J. Res. Dev. **45**, 89 (2001).

[21] Y. Q. Zhan *et al.* Phys. Rev. B **78**, 045208 (2008).

[22] C. Troadec, L. Kunardi, N. Chandrasekhar, Appl. Phys. Lett. **86**, 072101 (2005).

[23] W. Li *et al.* J. Phys. Chem. B **109**, 6252 (2005).

[24] L. D. Bell and W. J. Kaiser, Phys. Rev. Lett. **61**, 2368 (1988).

[25] H. Aziz, Z. D. Popvic, N. Hiu, A. Hor, G. Xu, Science, **283**, 1900 (1999).

[26] E. Knoesel, H. Hotzel, M. Wolf, Phys. Rev. B **57**, 12812 (1998).

[27] V. I. Arkhipov, E. V. Emelianova, Y. H. Tak, H. Bässler, J. Appl. Phys. **84**, 848 (1998).

[28] S. M. Sze, C. R. Crowell, G. P. Carey, E. E. LaBate, J. Appl. Phys. **37**, 2690 (1966).

[29] M. A. Lampert, P. Mark, *Current Injection in Solids*, Academic Press, New York (1970).

[30] P. E. Burrows *et al.* J. Appl. Phys. **79**, 7991(1996).

[31] A. Kahn, N. Koch, W. Gao, J. Polym. Sci. B 41, 2529 (2003).

[32] X. Jiang *et al.* Phys. Rev. Lett. **90**, 256603 (2003).

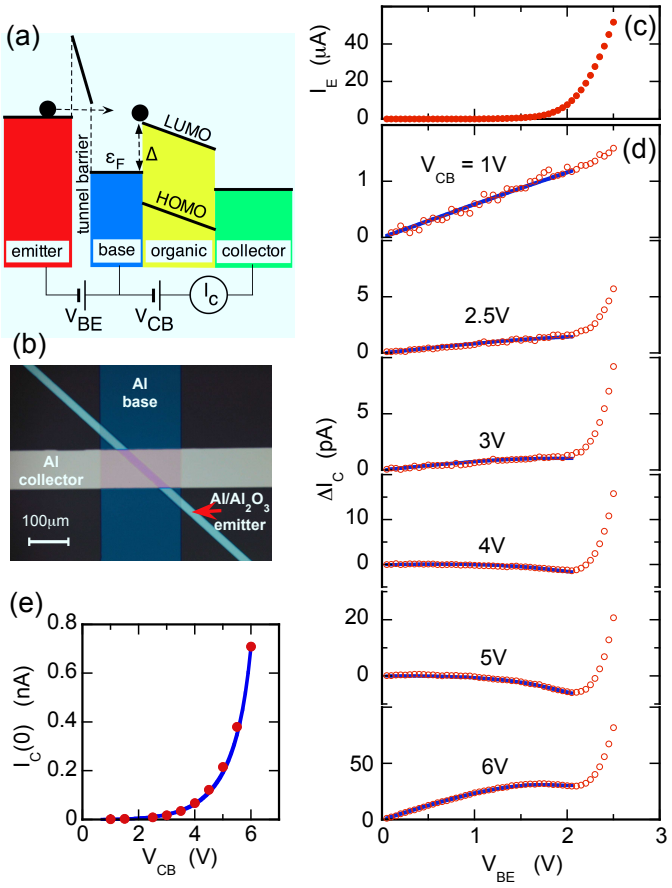

Figure 1
Jiang et al. "Direct Determination of Energy Level Alignment..."

FIG. 1. : (Color figure) (a) Schematic energy level diagram of BEES. (b) A photograph of an Al/Alq_3/Al device. (c) I_E and (d) ΔI_C at several values of V_{CB} are plotted against V_{BE}. The solid curves are fits described in the text. (e) $I_C(0)$ vs. V_{CB}. The solid curve is a fit to the Arkhipov model[27].

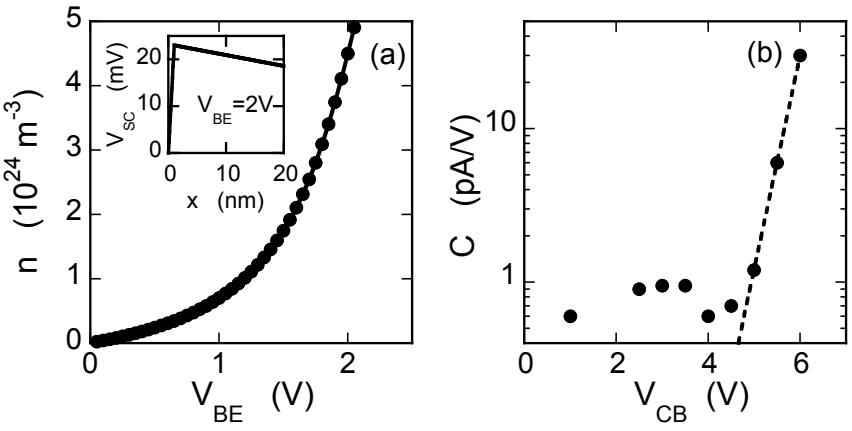

Figure 2
Jiang et al. "Direct Determination of Energy Level Alignment..."

FIG. 2. (a) Calculated n as a function of V_{BE} for the Al/Alq_3/Al device in Fig. 1. Inset: The position-dependence of V_{SC}. (b) The fitting coefficient C as a function of V_{CB}.

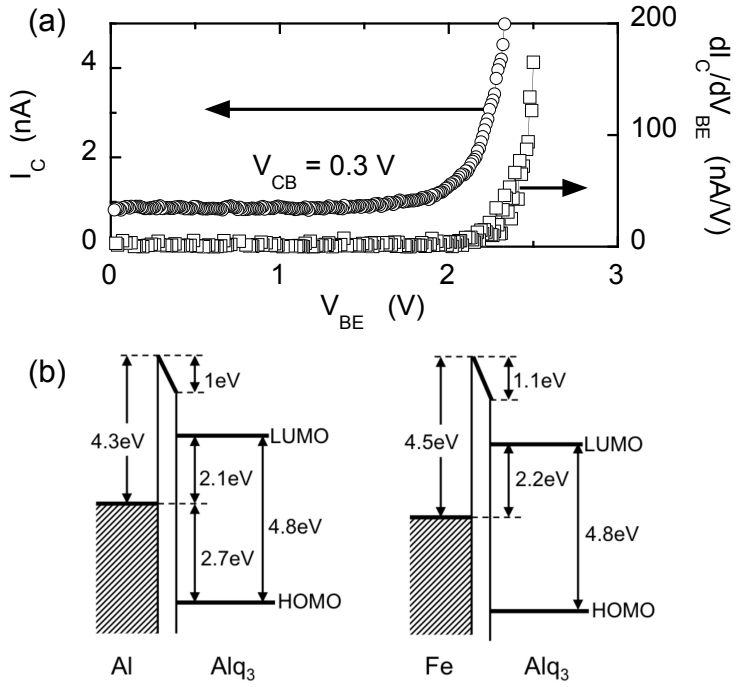

Figure 3
Jiang et al. "Direct Determination of Energy Level Alignment..."

FIG. 3. (a) I_C and dI_C/dV_{BE} vs. V_{BE} for an Fe/Alq_3/Au device. (b) Schematic diagrams of energy level alignment at Al/Alq_3 and Fe/Alq_3 interfaces.